DENTAL MATERIALS 35 (2019) 1545–1556

Available online at www.sciencedirect.com

ScienceDirect

journal homepage: www.intl.elsevierhealth.com/journals/dema

Ultrashort-pulse laser as a surface treatment for bonding between zirconia and resin cement

Mahmood Abu Ruja[a,b,c], *Grace M. De Souza*[a], *Yoav Finer*[a,b,*]

[a] *Faculty of Dentistry, University of Toronto, 124 Edward Street, Toronto, ON M5G 1G6, Canada*
[b] *Institute of Biomaterials and Biomedical Engineering, Faculty of Applied Science and Engineering, University of Toronto, Rosebrugh Building, Room 407, 164 College Street, Toronto, ON M5S 3G9, Canada*
[c] *Department of Prosthodontics, Faculty of Dentistry, Jordan University of Science & Technology (JUST), P.O. Box 3030, Irbid 22110, Jordan*

ARTICLE INFO

Article history:
Received 13 March 2019
Received in revised form
15 July 2019
Accepted 16 July 2019

Keywords:
Y-TZP
Surface characterization
Crystalline phases
X-ray diffraction analysis
Surface wettability
Surface roughness
Alumina blasting
Tribochemical silica coating
Microtensile bond strength
Thermocycling

ABSTRACT

Objectives. To evaluate ultrashort-pulse laser (UPL) as a surface treatment for improved bond strength to Yttria-tetragonal zirconia polycrystalline (Y-TZP).

Methods. Fully-sintered Y-TZP samples received either no treatment (CTL), or were treated by alumina blasting (ALB), tribochemical silica coating (SIL), or one of two UPL patterns: multiple pulses laser surface dots with 2.5 μm spacing (8 mJ, 10 kHz)(LSD); or single pulse laser surface lines with 2.5 μm spacing (4 mJ, 6.7 kHz)(LSL). Surface roughness, wettability (contact angle), and quantification of crystalline phases were evaluated for each group (n = 3/group). Y-TZP treated slabs were cemented to resin composite slabs using silane and 10-methacryloyloxydecyl dihydrogen phosphate (MDP)-containing adhesive. Beams from the Y-TZP/resin blocks were microtensile tested (n = 5/group) after 48 h water incubation (37 °C) with or without subsequent thermocycling (5–55 °C, 5000 cycles).

Results. All surface treatments increased surface roughness values versus control ($P < 0.001$). Contact angles were lowest for SIL (6.57 ± 2.37°) and highest for control (50.97 ± 6.30°). LSL and LSD were the only treatments that did not increase the relative monoclinic phase. All surface treatments significantly increased microtensile bond strengths (μTBS) compared with the control group ($P < 0.001$), with highest values for UPL (LSD: 35.40 ± 4.53 MPa > LSL: 31.84 ± 8.46 MPa > SIL: 19.95 ± 3.99 MPa = ALB: 19.51 ± 2.55 MPa > CTL: 14.51 ± 2.23 MPa). Thermocycling significantly reduced bond strength for all treatments in a surface treatment-dependent manner.

Significance. The ability of UPL to alter Y-TZP surface morphology, increase wettability and μTBS without increasing the monoclinic content suggests its potential to improve bonding to the underlying resin cement and tooth without compromising the strength of the restoration.

* *Corresponding author at*: Faculty of Dentistry, University of Toronto, 124 Edward Street, #551, Toronto, ON, M5G 1G6 Canada.
E-mail address: yoav.finer@dentistry.utoronto.ca (Y. Finer).

https://doi.org/10.1016/j.dental.2019.07.009

1. Introduction

Yttria-tetragonal zirconia polycrystalline (Y-TZP) is a promising ceramic material because of its biocompatibility, superior mechanical and optical properties [1–3]. Y-TZP has shown better mechanical performance, superior strength and fracture resistance than other ceramic materials with a flexural strength of more than 900 MPa, and fracture toughness of up to 10 MPa/$m^{0.5}$ [4,5]. While resin cements can be bonded successfully to tooth structure, Y-TZP has limited bond strength to the tooth because the limited adhesion between the cements and the restoration [6–8]. This is due to the lack of a glassy matrix in Y-TZP, which makes it an acid conditioning resistant ceramic [9], and the absence of SiO_2, which reduce its chemical bonding to silane coupling agents [10]. A strong bond is needed for long-term clinical success especialy when bonded restorations are considered such as resin-bonded fixed dental prosthesis (FDPs) and veneers [11]. This bond can be potentially improved by treating the surface of Y-TZP by other means than acids and silane agents [12,13]. Different surface treatments have been proposed to improve the bond strength to resin cements. These include: surface grinding [14,15]; airborne-particle abrasion using Al_2O_3 [16]; tribochemical silica coatingh [17]; or specific primers [18]. However, no benchmark has been established to date [19].

Laser (*Light Amplification by Stimulated Emission of Radiation*) was suggested as an alternative method for ceramic surface treatment because of its potential to alter the surface in a more controlled manner than traditional methods [20,21]. Previous works have investigated the ability of different types of lasers to increase the surface roughness of zirconia [22,23]. However, surface destruction and phase transformation due to thermal effects of high-power lasers have raised concerns regarding its usability [23]. Recent advancements in laser technology resulted in the development of the ultrashort pulsed laser (UPL) [24], which includes an effective reduction of surface irradiation energy that potentially does not induce any thermal or mechanical damage to the surface [25,26]. Therefore, using UPL to increase surface roughness and consequently bond strength of zirconia substrates while preserving surface properties may be an alternative to conventional treatments of the surface such as alumina blasting (ALB) and tribochemical silica coating (SIL). However, very limited research has been done in this area. Therefore, the effect of UPL on zirconia surface characteristics (i.e. surface roughness, energy, crystalline structure) and its bond strength to resin cements need further exploration.

The aims of this study are to: (1) Characterize the effect of UPL on Y-TZP surface morphology, surface energy, and phase transformation, and to compare the effect of UPL with conventional surface treatments ALB and SIL; (2) Assess the effect of UPL surface treatment on Y-TZP bond strength to resin cement before and after thermocycling and compare it to ALB and SIL.

We hypothesize that: (1) UPL surface treatments will alter surface roughness, and increase wettability of Y-TZP substrates in comparison to other treatments (ALB and SIL), without affecting the crystalline content on the surface; (2) UPL will improve the bond strength between Y-TZP and resin cement in comparison to traditional surface treatments (ALB and SIL).

2. Material and methods

Materials used in the study are listed in Table 1. To address the research objectives, the project was conducted as follows:

2.1. Y-TZP slabs preparation

Pre-sintered Y-TZP blocks (Lava™ Plus, 3M ESPE, St Paul, MN, USA) were cut and prepared into slabs using a diamond wafering blade (Isomet 1000 Low-Speed Saw, Buehler Ltd., Lake Bluff, Illinois). Y-TZP slabs were sintered in a high-temperature furnace (Lava™ Furnace, 3M ESPE, Seefeld, Germany) according to the manufacturer's recommendations, where the temperature was raised and kept at (1450 °C) for 2 h. The final measurements for the fully sintered Y-TZP slabs were 4 × 8.8 × 8.8 mm.

2.2. Y-TZP slabs surface treatment

Samples' surfaces were grounded with silicon carbide paper up to 600 grit, then ultrasonically cleaned for 10 min in distilled water (FS5 Fisher Scientific, Sheboygan, Wisconsin, United States), and air-dried. Subsequently, Y-TZP slabs were randomly distributed into five groups (n = 5/group) according to the surface treatment: (1). **CTL** (control group; no surface treatment) (2). **ALB** (alumina blasting), (3). **SIL** (tribochemical silica coating), (4). **LSD** (Ultrashort pulsed laser ablation/Dots pattern), or (5). **LSL** (Ultrashort pulsed laser ablation/Lines pattern) (Fig. 1).

2.2.1. Alumina blasting (ALB), group 2

Samples were blasted with 50 μm aluminum oxide (Al_2O_3) particles at 2.5 bar for 15 s, with the tip being held at a 10-mm distance and inclined at approximately 45° [20,27,28]. After alumina blasting, samples were cleaned using an air stream to remove any remnants of alumina particles on the surface.

2.2.2. Tribochemical silica coating (SIL), Group 3

Samples were blasted with 30 μm silica-coated alumina particles (Cojet sand, 3M ESPE, Neuss, Germany) at 2.5 bar for 15 s, with the tip being held at a 10-mm distance and inclined at approximately 45° [20,27,28]. After treatment, samples were cleaned using an air stream to remove any remnants of particles on the surfaces.

2.2.3. Ultrashort pulsed laser (UPL), Groups 4 and 5

The zirconia surface was irradiated with a solid-state Neodymium-doped yttrium orthovanadate (Nd:YVO_4) ultrafast laser (Lumera, Hyper Rapid 50, Coherent, USA), with 1064 nm fundamental output wavelength, and 10 picoseconds (ps) pulse duration. Samples were attached to a computer-controlled XYZ-motorized stage.

Two laser patterns were applied:

1 LSD (Group 4): dots pattern, with 2.5 μm spacing between dots in any direction, 8 mJ, 10 kHz, multiple pulses.

Table 1 – Description of the materials used in this study.

Material	Composition	Lot number	Manufacturer
Lava™ Plus	Tetragonal polycrystalline zirconia partially stabilized with 3mol-% Yttria	520217	3M ESPE
CoJet™ System Sand	Silicatized sand (particle size 30 μm)	620599	3M ESPE
Blasting Compound	Aluminum Oxide (particle size 50 μm)	1629071	Ivoclar Vivadent Inc.
Filtek™ Z250	-TEGDMA (triethylene glycol dimethacrylate) -UDMA (urethane dimethacrylate) -Bis-EMA (Bisphenol A polyetheyleneglycol diether dimethacrylate)	N736805	3M ESPE
RelyX™ Ultimate	Methacrylate monomers, Filers, Initiator, Dark cure activator for Scotchbond Universal	618736	3M ESPE
Scotchbond™ Universal	MDP phosphate monomer, Silane, Vitrebond copolymer	613345	3M ESPE

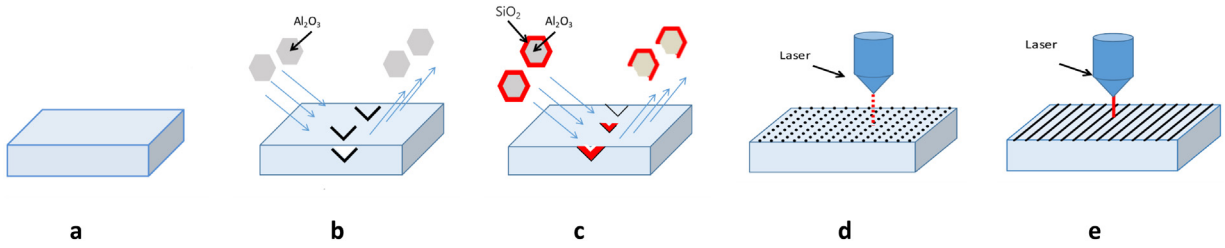

Fig. 1 – Y-TZP slabs surface treatment groups: (a) CTL (no surface treatment); (b) ALB (samples were alumina blasted with 50 μm aluminum oxide (Al_2O_3); (c) SIL (samples were blasted using 30 μm silica-coated alumina particles); (d) LSD (dots pattern, with 2.5 μm spacing between dots in any direction created using Nd:YVO_4 ultrafast laser); (e) LSL (lines pattern with 2.5 μm spacing between lines created using Nd:YVO_4 ultrafast laser).

2 LSL (Group 5): lines pattern, with 2.5 μm spacing between lines, 4 mJ, 6.7 kHz, single pulse.

After UPL ablation, samples were ultrasonically cleaned to remove any surface debris for 10 min in distilled water (FS5 Fisher Scientific, Sheboygan, Wisconsin, United States), and air-dried.

2.3. *Surface characterization*

Y-TZP slabs' surfaces were characterized as follows:

2.3.1. *Surface roughness analysis*

A three-dimensional analysis of the surface topography was done using surface profilometer (P-16+ Profiler, KLA-Tencor Corporation, Milpitas, CA, USA). Three areas (0.2*0.2 mm each) were characterized for each specimen (n = 3/group). The average roughness values (Sa) were measured using compatible software (Apex Software).

For qualitative analysis, selected specimens were examined using Scanning Electron Microscope (SEM) at 200×, and 2000 × magnification (6610 Scanning Electron Microscope, JEOL Ltd., Japan), at a low vacuum level, operating voltage of 15 kV, and a working distance of 10 mm.

Energy-dispersive X-ray spectroscopy (EDS) analysis was performed (6610 Scanning Electron Microscope, JEOL Ltd., Japan) to evaluate the availability of chemical components at 500× magnification [29].

2.3.2. *X-ray diffraction analysis (XRD)*

A diffraction analysis was conducted using a Philips XRD system, including a PW 1830HT generator, operated at 40 kV and 40 mA in the 2θ range of 25–65° to determine the effect of treatments on the crystalline phase content in the samples [30]. A quantitative value of phase composition of specimens (the relative monoclinic phase) was obtained using Reference Intensity Ratio (RIR) analysis (X'Pert Quantify, PANalytical, Almelo, Netherlands) after matching the sample patterns (n = 3/group) with a reference pattern (ICDD pdf4+) [31].

2.3.3. *Contact angle*

The degree of wetting (wettability of specimen surfaces was determined using water contact angle measurement [32] with a goniometer (NRL C.A. goniometer, Ramé-Hart, Inc., Mountain Lakes, NJ, USA). A microsyringe was used to place a 20 μL droplet of distilled/deionized water on the surface of each sample. Five droplets were deposited on the surface of each sample and measured individually. For each droplet, the contact angle was measured on two opposite sides using a microscope at 300× magnification and the average was reported as a single measurement. Five measurements were acquired per sample (n = 3/group).

2.4. *Microtensile bond strength*

2.4.1. *Composite slabs preparation*

Composite slabs (4 × 8.8 × 8.8 mm) were prepared from resin composite (Filtek™ Z250, shade A1, 3M ESPE, St Paul, MN, USA). In order to standardize the shape and dimensions and surface roughness of the slabs, the following protocol was followed:

A clear silicone impression of the Y-TZP slabs was taken and used as a mold for reproducing its shape. Composite resin layers were incrementally condensed into the mold and

light-cured for 40 s on each side at 650 mW/cm^2 (Demi curing light curing system, Kerr, Orange, CA, USA). The light intensity was confirmed with a radiometer (Optilux, model 200, Kerr, Orange, Calif., USA) [33]. Composite slabs were then aged in water at room temperature (~22 °C) for at least 30 days to provide hydration. Surfaces were roughened with sequential silicon carbide paper up to 600 grit under water cooling, then cleaned in distilled water in an ultrasonic bath for 10 min (FS5 Fisher Scientific, Sheboygan, Wisconsin, United States).

2.4.2. *Cementation procedure*

The bonding surfaces of the Y-TZP slabs and composite resin slabs were treated according to the manufacturers' recommendations, as follows:

A silane and 10-methacryloyloxydecyl dihydrogen phosphate (MDP)-containing adhesive (Scotchbond™ Universal Adhesive, 3M ESPE, St Paul, MN, USA) was applied on each slab's surface for 20 s using a microbrush and left uncured. Resin cement (RelyX ™ Ultimate, 3M ESPE, St Paul, MN, USA) was applied to the Y-TZP surface with a mixing tip, the composite slab was placed on top of the Y-TZP/resin cement, and a compressive load of 6 N was applied. Excess of resin cement was removed with a microbrush, and the specimen was light-cured for 20 s on each side at 650 mW/cm^2 (Demi curing light curing system, Kerr). Cemented samples were stored for 24 h in distilled water.

2.4.3. *Microtensile beams preparation*

After storage, composite resin/Y-TZP blocks (8 × 8.8 × 8.8 mm) were sectioned using a water-cooled diamond wafering blade (Isomet 1000 Low-Speed Saw, Buehler Ltd.) into serial slices of 1 mm thickness, which were perpendicularly sectioned again into beams of 1.0 × 1.0 mm adhesive interface. In all blocks, the periphery cuts (±1.0 mm) were discarded to avoid interference of excess of resin cement on bond strength results.

Microtensile beams were stored for 48 h in distilled water at 37 °C and then either immediately tested (baseline) or tested after thermocycling for 5000 cycles (Thermocycler THE-1100, SD MECHATRONIK GMBH, Germany). Each cycle consisted of 20 s in 5 °C (cold bath) and 20 s in 55 °C (hot bath) with a dwell time of 10 s (ISO/TS 11,405:2015).

2.4.4. *Microtensile bond strength (μTBS) testing*

The beams were tested (N = 5/group) as follows:

Each beam was placed in a Bisco microtensile testing jig (BISCO Inc., IL, U.S.A.) and stabilized using cyanoacrylate glue (Zapit BASE, Dental Ventures of America, Inc.) with an accelerator (Zapit Accelerator, Dental Ventures of America, Inc.). The jig containing the sample was carefully installed in a microtensile tester (BISCO Inc., IL, U.S.A.) and a tensile load was applied at a crosshead speed of 0.5 mm/min until failure occurred. Load at failure and the cross-sectional dimension of each sample were recorded to determine microtensile bond strength in MPa.

2.4.5. *Mode of failure*

To determine the mode of failure, all specimens were observed after testing under a stereomicroscope (Wild/Leica M3Z Stereo Microscope, Heerbrugg, Switzerland) at ×50 magnification. The failure modes were classified as: A = adhesive failure at the zirconia–cement interface; B = cohesive failure in cement; C = mixed A and B.

2.5. *Data analyses*

Sa values, relative monoclinic phase values, and contact angle values were analyzed by one-way ANOVA and Tukey's test ($\alpha = 0.05$).

Microtensile bond strength values (μTBS) were analyzed with two-way ANOVA and Tukey's test ($\alpha = 0.05$), with surface treatment and storage being the independent variables and bond strength value as the dependent variable.

Failure modes were analyzed using chi-square test of independence, with a confidence level of 95% [34,35].

Number of specimens in each experimental group was selected according to preliminary data and the literature, providing sufficient power ($1\text{-}\beta = 0.8$) to detect a difference of ~20% ± 10% ($p < 0.05$) [34,35].

3. Results

3.1. *Surface characterization*

All surface treatments significantly ($P = 0.001$) increased surface roughness (Sa) compared to CTL (0.22 ± 0.05 μm) (Mean ± SD) (Fig. 2a). The Sa values for LSD (0.53 ± 0.04 μm) and LSL (0.54 ± 0.03 μm) were not significantly different from ALB (0.56 ± 0.19 μm). SIL treated samples presented intermediary Sa values (0.39 ± 0.06 μm), which were different from the other surface treatments ($P = 0.02$), but were significantly ($P = 0.003$) higher than the CTL samples.

Analysis of X-ray diffraction patterns of Y-TZP surfaces (Fig. 2b) showed that CTL group has tetragonal phase on the surface. Surfaces treated with either SIL or ALB presented an increase in the monoclinic phase content: ALB treated samples showed a relative monoclinic phase content of 29.33 ± 2.52 vol.% ($p < 0.001$), and SIL treated samples presented approximately 26 ± 2.00% of relative content of monoclinic phase ($p < 0.001$). In contrast, when samples were treated with either LSD or LSL, a similar content of tetragonal phase to that of the control was observed.

Degree of wetting for the different surface treatment is depicted in Fig. 2c. Contact angle (Fig. 2c) were the lowest for SIL treated samples ($P < 0.001$), followed by LSL and LSD ($P < 0.05$), then ALB ($P < 0.05$), and were highest for CTL ($P < 0.001$) (SIL: 6.57 ± 2.37° < LSL: 13.70 ± 1.24° = LSD: 16.80 ± 0.96° < ALB: 20.64 ± 4.45° < CTL: 50.97 ± 6.30°).

SEM observations of specimens' surface after the various treatment are depicted in Fig. 3 . CTL samples show a relatively smooth surface lacking any irregularities compared to the other groups (a1). Shallow straight-line grooves appeared on high magnification (a2) were resulted from polishing with silicon carbide abrasive paper (600 grit). The valleys formed in ALB appear larger compared to SIL (compare b1 and b2 with c1 and c2). ALB (b1, b2) and SIL (c1, c2) treated samples show irregularly roughened surfaces, versus the more regularly roughened surfaces for the LSD (d1, d2) and LSL (e1, e2). Well-distributed and uniform undercuts are visible for LSD and LSL treated groups. (d1, d2, e1, e2). LSL resulted with

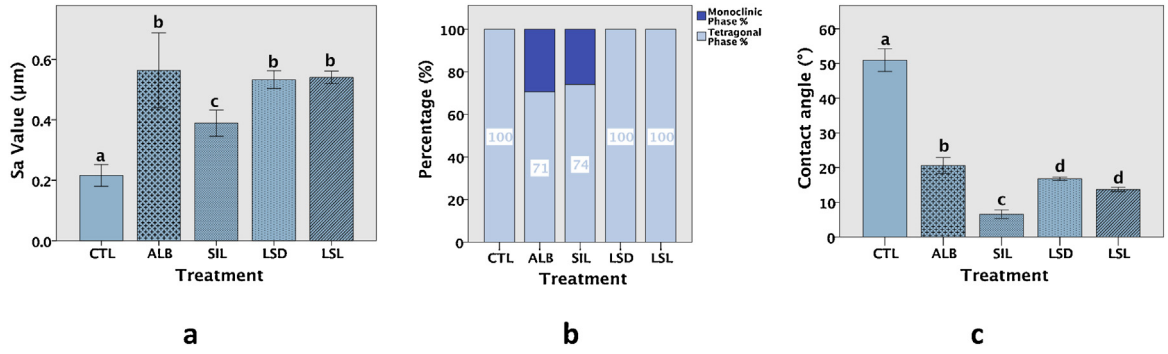

a b c

Fig. 2 – (a) Bar graph illustrating a significant increase in mean surface roughness values (Sa) for all surface treatments compared to the control ($p < 0.05$); values for SIL are significantly lower compared with other surface treatments ($p < 0.05$). (b) Bar graph illustrating analysis of the crystalline phase content of the surface. CTL, LSD, and LSL groups maintained the tetragonal crystalline phase, while ALB and SIL induced a monoclinic phase on the surface by 29% and 26% respectively. (c) Bar graph illustrating the mean contact angle (°). All surface treatment significantly reduced the contact angle compared to CTL. SIL resulted with the lowest value ($p < 0.001$). Different letters represent a significant difference between groups ($p < 0.05$).

continuous relatively uniform parallel line pattern over the surface (e1, e2), while LSD was less uniform and continuous (d1, d2).

Atomic composition evaluated by energy-dispersive x-ray spectroscopy (EDS) for CTL (a), ALB (b), and SIL (c) groups is depicted in Fig. 4. Al particles found on both ALB and SIL groups were remnant of the alumina particle blasting (Fig. 4 b, c), and confirmed the presence of silica over SIL surfaces (Fig. 4c). However, deboned SIL treated surfaces had no silica on the Y-TZP surfaces after thermocycling (data not shown).

3.2. *Bond strength*

The results of the micro tensile bond strength (μTBS) for the different groups are depicted in Fig. 5. Surface treatment or aging conditions (±thermocycling) significantly affected μTBS ($P < 0.001$). In addition to individual effects, there was a significant interaction between surface treatment*thermocycling ($P < 0.001$), indicating a surface treatment-dependent effect of thermocycling on the bond strength.

At baseline storage (48 h), LSL (39.48 ± 3.54 MPa) and LSD (39.18 ± 1.96 MPa) showed a significantly ($P < 0.001$) higher μTBS compared to other groups. After thermocycling, LSD (31.62 ± 2.55 MPa) was ranked significantly the highest, and were higher than LSL (24.19 ± 1.63 MPa) ($P < 0.001$). SIL (23.11 ± 2.60 MPa) and ALB (21.14 ± 2.28 MPa) was significantly higher than CTL (15.62 ± 2.75 MPa) at baseline ($P < 0.03$). After thermocycling, ALB (17.87 ± 1.66 MPa) was still significantly higher than CTL (13.41 ± 0.78 MPa) ($P = 0.007$), but no statistical difference was reported between SIL and CTL (16.80 ± 2.02 MPa) ($P = 0.06$).

3.3. *Mode of failure*

The modes of failure described in Table 2. There were significant differences between the mode of failure for all groups ($P < 0.001$) with a total of mixed failures = 58%, cohesive = 24%, and adhesive = 18%.

For all groups combined, thermocycling had no significant effect on the mode of failure ($P = 0.33$), with the mixed failure mode being predominant before thermocycling (mixed = 60%, cohesive = 27%, adhesive = 14%), and after thermocycling (mixed = 56%, cohesive = 21%, adhesive = 23%) ($P < 0.001$). Individual analyses for each treatment group reveal no significant effect for thermocycling on CTL, ALB, LSD and LSL ($P > 0.05$), with mixed mode dominancy ($p < 0.05$). Thermocycling affected only SIL, with a predominant mixed failure mode before thermocycling (60%) ($P = 0.04$), however there were no significant differences between the failure modes after thermocycling for this group ($P = 0.25$).

4. Discussion

Y-TZP has superior strength, toughness, fatigue resistance and potentially enhanced long-term viability over other ceramics [1]. These factors make Y-TZP a suitable material for dental applications. However, despite its high mechanical properties, Y-TZP has compromised bond strength to the underlying substrate compared to other dental ceramics [21]. The long-term success of Y-TZP-based bonded restorations depends to a great extent on the adhesion between zirconia and resin cement and the underlying tooth substrate [36]. Therefore, the type of cement [37] and luting procedure [38] are important factors to consider. The materials in this study were selected because they are typical representatives of their categories, have been extensively investigated, thus providing a relevant and validated benchmarks for comparison, and allow for generalization of the results to similar materials that were not specifically tested in this study [39–43].

Alumina particles (Al_2O_3) (ALB) and tribochemical silica coating (SIL) were used as reference groups for surface treatment in comparison with the experimental groups composed of ultrashort pulsed laser treatment (LSD, LSL). To standardize the technique and reduce variability, the distance of the alumina blasting instrument, blasting pressure and time were maintained as constants through all air abrasion protocols.

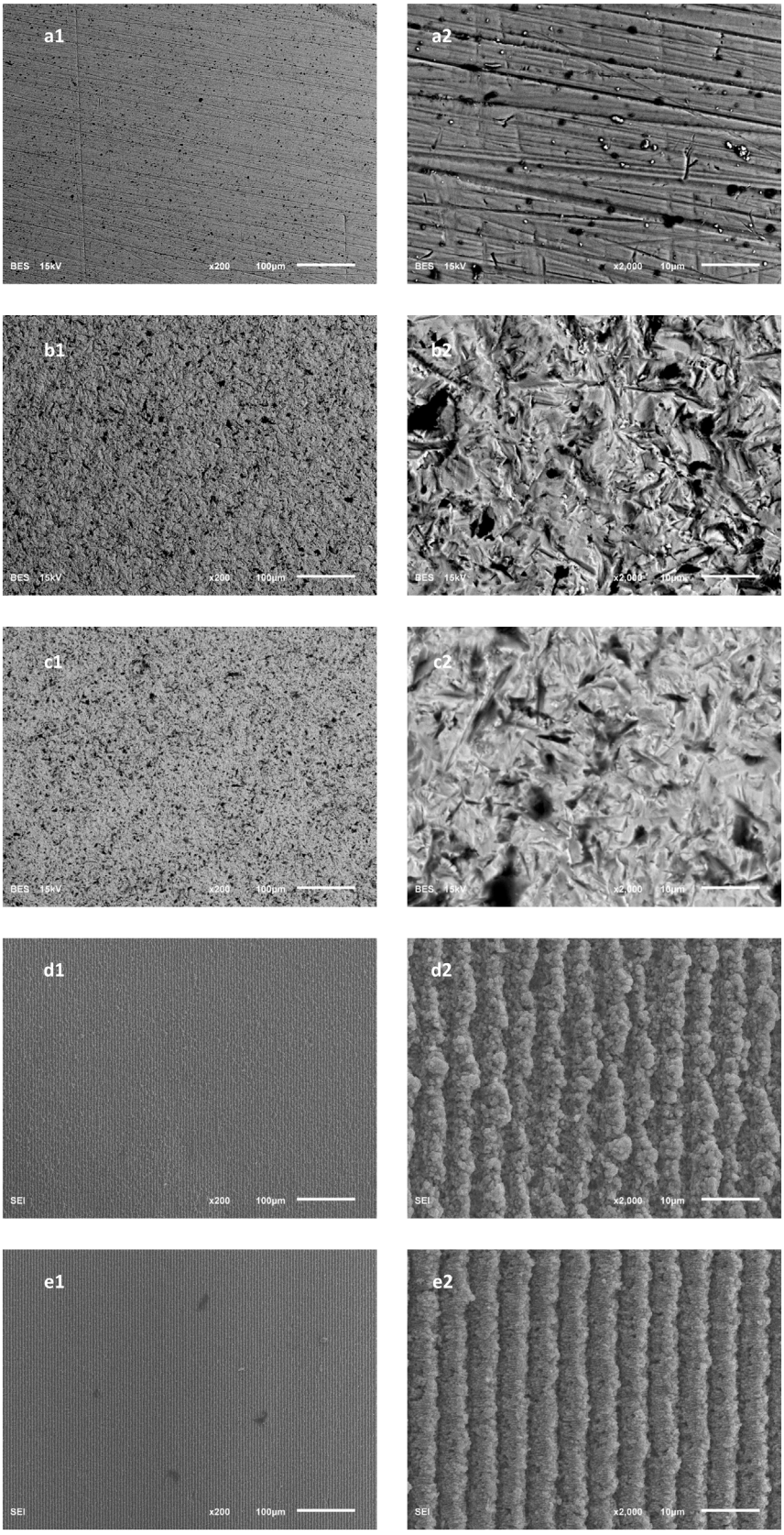

Fig. 3 – SEM micrographs for surface treatments; left column ×200 original magnification, right column ×2000 original magnification. CTL samples (a1) show a relatively smooth surface lacking any irregularities compared to the other groups. The valleys formed in ALB were larger compared to SIL (compare b1 and b2 with c1 and c2). ALB (b1, b2) and SIL (c1, c2) show irregularly roughened surfaces, versus the more regularly roughened surfaces for LSD (d1, d2) and LSL (e1, e2).

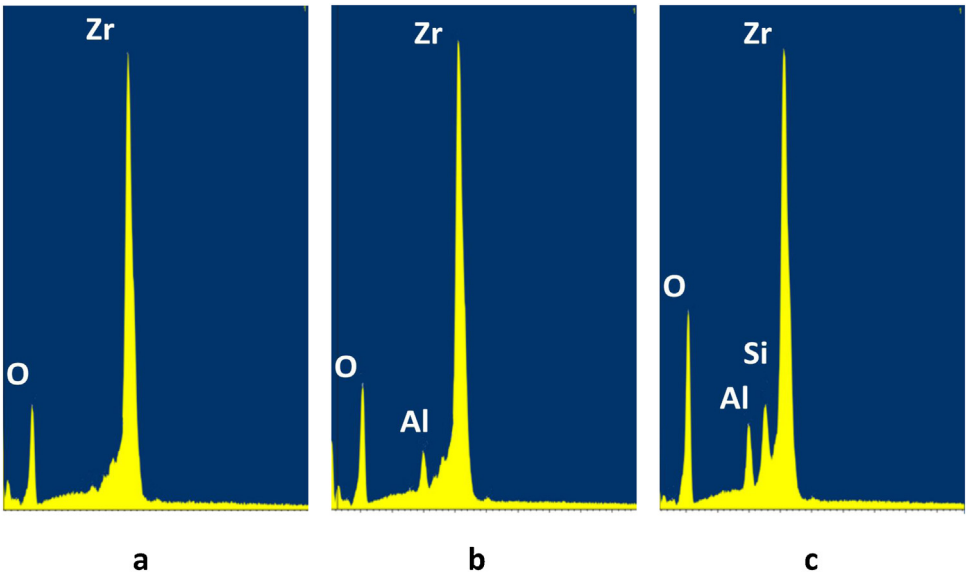

Fig. 4 – Atomic composition evaluated by energy-dispersive x-ray spectroscopy (EDS) for CTL (a), ALB (b), and SIL (c) groups. EDS confirmed the presence of Si on the surface of SIL samples. Al particles found on both ALB and SIL groups are remnant from alumina blasting.

Table 2 – Failure mode of Y-TZP samples after microtensile bond strength testing.

Treatment	48 h storage						48h + thermocycling						
Type of failure	CTL	ALB	SIL	LSD	LSL	Sub-total	CTL	ALB	SIL	LSD	LSL	Sub-total	Total
Adhesive failure	27%[a]	20% [a]	7% [b]	7% [a]	7% [b]	14% [b]	47% [a]	27% [a]	20% [a]	7% [b]	13% [b]	23% [b]	18% [b]
Cohesive failure	0%	27% [a]	33% [b]	40% [a]	33% [b]	27% [b]	0%	33% [a]	27% [a]	27% [b]	20% [b]	21% [b]	24% [b]
Mixed failure	73% [a]	53% [a]	60% [a]	53% [a]	60% [a]	60% [a]	53% [a]	40% [a]	53% [a]	66% [a]	67% [a]	56% [a]	58% [a]

* Different subscript letters represent a significant difference between mode of failure within the same treatment subgroup, total groups, and subtotal groups combined before or after treatment ($P < 0.05$).

The most frequently used values were reproduced: distance of 10 mm from the surface [20,27,44]; particles' size of 30 μm for the Cojet™ sand [20,27,45,46], and 50 μm for the alumina particles sand [27,47]; blasting time of 15 s [20,27,46]; and a pressure of 2.5 bar [28,48].

While ALB and SIL have already been intensively studied [20,27,28,46], there remain several disadvantages inherent to the application of those particles: irregular patterns of roughness created on the zirconia surface, the formation of microcracks, and a considerable amount of phase transformation from tetragonal to monoclinic are outcomes that have been reported [49]. Surface cracks generated on the surface of zirconia may develop into severe stress intensifiers when exposed to a wet environment under cyclic loading [50]. A decrease in strength of 30% during contact fatigue testing after alumina blasting was indeed reported by Zhang et al. [51]. This was explained by the formation of surface microcracks larger than 4 μm, which under sustained loading would grow and promote radial crack initiation [52].

Ultrashort pulsed laser in the form of lines (LSL) or dots (LSD) were used as possible alternatives to the mechanical blasting of the zirconia surface with alumina particles. Several laser parameters and patterns were applied in a preliminary study and compared by means of contact angle, surface roughness, and surface morphology to determine the laser protocol that created values close to the conventional ALB and SIL treatments, but without the latter's treatments surface destruction. This resulted in the selection of the two patterns presented here, LSL and LSD. The most important effect of the laser is to convert radiant energy to heat (the thermo-mechanical effect). The energy of the laser beam is absorbed by the surface and creates a heat induction process that produces shell-like ruptures on the ceramic surface [53].

All surface treatments resulted in increased surface roughness in comparison to the untreated surfaces (CTL), with Sa values similar for LSL, LSD, and ALB, that were higher than SIL. The higher Sa value for ALB versus SIL could be the results of the former use of bigger particles (50 μm) compared with the size of the latter (30 μm). SEM observations support the above

Well-distributed and uniform undercuts are visible for LSD and LSL treated groups. (d1, d2, e1, e2). LSL resulted with continuous parallel line pattern over the surface without significant interruptions (e1, e2), while LSD was less continuous and uniform (d1, d2).

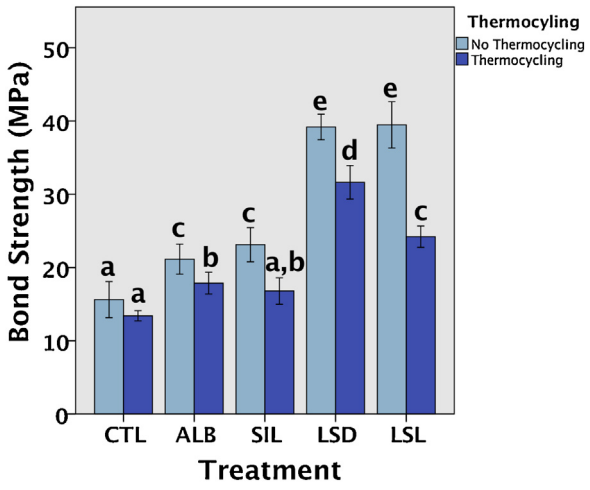

Fig. 5 – Bar graph illustrating mean zirconia-composite micro-tensile bond strength values (μTBS). Different letters represent a significant difference between groups ($p < 0.05$). Surface treatment or aging conditions (±thermocycling) significantly affected μTBS ($P < 0.001$). There was a significant interaction between surface treatment*thermocycling ($P < 0.001$). The control group (CTL) exhibited lower μTBS values than the other groups ($p < 0.001$). At baseline storage (48 h), LSL and LSD showed a significantly higher μTBS compared to SIL and ALB ($p < 0.001$). After thermocycling, the bond strength values were reduced significantly for all treatments ($p < 0.001$).

findings; overall, the surfaces of ALB and SIL treated groups were characterized by irregular and non-uniform notches created by the impact of the sharp alumina particles. However, because alumina blasting is manually applied, the lack of absolute uniform control results in some variation of indentation depths throughout the surface. In contrast, both UPL patterns (LSL and LSD) were relatively uniform. A regular pattern of engraving was achieved with the laser treatment since the depth, width, and pattern of the surface can be prepared and managed using a computer-aided machining with a designated software.

To test bonding effectiveness, zirconia slabs were cemented in this study to composite resin slabs [54]. The main purpose of this sample design was to create a uniform rather than the heterogeneous structure of tooth enamel and dentin, allowing for a more precise interpretation of bond strength values [55]. By using resin composite as a substrate, the zirconia/resin cement interface was challenged rather than the stronger resin-based cement/composite resin interface, thereby evaluating the effect of different Y-TZP surface treatments on its potential to be bonded to tooth structure. Adhesive resin cement combined with silane and MDP-containing adhesive were used, as the application of such adhesive resulted in an increase of the bonding effectiveness to zirconia, as indicated by a higher μTBS [43,56]. A reaction may be formed between the di-valent phosphoryl groups of MDP monomer and hydroxyl groups on the zirconia surface [57].

All surface treatments resulted in increased μTBS values after aging compared with the control samples. For ALB, this was likely due to the roughened zirconia surface produced after alumina blasting, which would potentially increase the bonding surface area, increase surface energy and improve wettability [58], thus allowing for micromechanical interlocking of the resin cement. However, several disadvantages inherent to these particles include: the irregular patterns of roughness created, the formation of microcracks, and a considerable phase transformation from tetragonal to monoclinic as a consequence of alumina blasting [49].

SIL was introduced to roughen the surface similarly to ALB, while promoting silane-mediated chemical bond [59]. The silica deposited on the surface resulted in a significantly lower contact angle, which indicates a potential for better wettability by the adhesive agents applied, as well as a chemical interaction between the silane coupling agent available in the adhesive and the silica-impregnated layer [60,61]. Yet, similar bond strength values were observed in the current study for ALB and SIL groups at baseline. This could be due to the fact that the silica particles are not impregnated on the surface and are rather deposited in loose clusters, resulting in lower than expected bond strength [28]. It can be suggested therefore that the aforementioned chemical bond does not contribute significantly to the overall bond strength, because the particles that provide this bond are not strongly attached to the surface and that surface roughness, may play a more significant role.

Several studies have shown that the UPL can provide a precise zirconia surface treatment without generating excessive heat. In addition, this technique can ablate material into a thin surface layer without disturbing the material properties [62]. Although the measured roughness values for LSL and LSD in this study are similar to ALB, SEM showed a more uniform surface patterns following LSD and LSL, unlike ALB and SIL, as a result of the controlled engraving described above. This well-controlled and regular surface pattern facilitated the creation of retentive grooves and undercuts, visible in the SEM images, which could explain the higher bond strength values after UPL treatments. This is corroborated by previous studies which have demonstrated that an increase in bond strength is related to the presence of undercuts in zirconia laser-irradiated groups [63,64]. In contrast, lower levels of undercuts were reported for airborne-particle abrasion methods, such as ALB and SIL [60,65], providing a possible explanation for the lower bonds values found in the current study for these surface treatment versus UPL treatment.

ALB and SIL treated samples presented higher relative monoclinic content than all the other groups. It has been reported that alumina blasting results in the generation of microcracks in the surface of zirconia [49]. In the surrounding zones of a propagating crack, tetragonal crystals may transform into their stable monoclinic structure [66]. Since this transformation is accompanied by a 3–4 % volume expansion, the stresses induced by the transformation lead to the formation of a zone with large compressive stresses that can partially close the crack and slow down its propagation, increasing the material toughness [51,67]. Although this localized phenomenon has a protective effect, others argue that the tetragonal-to-monoclinic phase transformation would potentially reduce the mechanical properties [68], and might

compromise the lifetime of zirconia [69]. Therefore, the ability of LSD and LSL to maintain the tetragonal crystalline phase of the Y-TZP surface stable after treatment can be considered as a major advantage. This indicates that these treatments were able to regularly roughen the surface and improve bonds strength without generating cracks and stresses at the surface and sub-surface layers. This is in line with findings of Fielder et al. [70], who studied ceramics machining using femtosecond laser and concluded that femtosecond laser pulses provide promising advantages in comparison with classical abrasive surface treatments as the first offers precise machining with a small influence on the materials' integrity. Their findings also revealed a surface that did not show any evidence of material degradation such as micro-cracks [26].

To assess the long-term bond strength, thermocycling was performed to simulate thermal changes that occur in the mouth and act as a fastened aging process [71,72]. Samples were subjected to 5000 thermal cycles between 5 and 55 °C as previously suggested for mimicking oral conditions [3,71]. Thermocycling significantly reduced bond strength for all treatments applied. Thermal stresses introduced by temperature changes in the thermocycling process may amplify the coefficient of thermal expansion mismatch of the bonded materials, which generates mechanical stresses at the bonded interface, resulting in strength degradation [73]. The significant decrease of the μTBS in aged condition could be also attributed to hydrolytic degradation of the interface components due to forced water penetration [74,75]. Thermocycling affected all surface treatment groups, but not the control, suggesting that the rougher surfaces are more susceptible to thermo-mechanical stresses [38]. The significant treatment * thermocycling effect indicates a surface treatment-dependent effect of thermocycling on the bond strength. For specimens that were not thermocycled, both SIL and ALB resulted in a significantly higher μTBS compared to the control with no differences between the surface treatment groups. After thermocycling, while the bond strength of ALB remained significantly higher than CTL, bond strength for SIL decreased and showed no significant difference to CTL. This suggests that that the bonding mechanism by SIL is more susceptible to thermal and thermomechanical stresses, perhaps due to an instability of the silane-mediated bonds and/or due to a loose connection between silica particles and zirconia surface [28]. This was further confirmed by EDS mapping for the debonded SIL treated surfaces that confirmed the absence of silica over the Y-TZP surfaces after thermocycling. These results are consistent with Kern and Wegner [76], and Blatz et al. [77], who concluded that ALB followed by MDP application provides superior long-term bond strength than silica-coated zirconia bonded to resin cement.

The significant treatment * thermocycling effect is further demonstrated for LSD and LSL. Although both patterns resulted in the highest initial μTBS values, LSL suffered from a greater reduction in bond strength after thermocycling compared with LSD. This could be due to the pattern created on the treated surface; the unifomr continuous lines (or channels) may have made it easier for the water to penetrate through the interface during aging, increasing the exposed surface area for water. This phenomenon could be exacerbated by the presence of hydrophilic resinous material (silane and MDP-containing resin) over the zirconia-resin interface that attract water to the bonded interface, thus weakens the interfacial bond due to hydrolysis [75].

The modes of failures in this study after μTBS testing show dominancy of mixed mode failure before thermocycling for all treatments. The mixed type of failure in this study was characterized by remnants of cement tending to remain attached to the corners of the bonded interfaces, suggesting that stresses are more concentrated at the central area of the adhesive interface. This is in line with the finite element analysis study carried out by Phrukkanon et al. [78], who found that stresses were concentrated at the central region of samples. After thermocycling, while the mixed type of failure was still dominant for CTL, ALB, LSD, and LSL, it ceased to be the dominant failure mode for SIL. This change in mode of failure for SIL could be related to this groups higher hydrophilicity of the interface compared with the other treatments in this study, indicated by the contact angle results, that could have increased the susceptibility of the SIL group to hydrolytic degradation of the interface [74], and thermal stresses introduced by temperature changes, that led to detachment of the SIL blasting particles [73]. This is in agreement with De Souza et al. [29], who reported a similar increase in the adhesive mode of failure after aging.

5. Conclusions

Within the limitation of our study, we conclude that:

1 Surface treatments significantly increased the Y-TZP surface roughness and surface wettability.
2 Y-TZP surface treatments significantly increased the μTBS to resin cement.
3 LSD provided the highest bond strength of Y-TZP to resin cements.
4 UPL uniformly increased the surface roughness, without inducing cracks or crystalline phase (t-m) transformation.
5 ALB and SIL treatments increased the monoclinic crystalline phase.
6 Thermocycling reduced bond strength for all groups, in a surface treatment dependent manner.

Based on the above, the hypotheses that UPL surface treatments will alter surface roughness, and increase wettability of Y-TZP substrates in comparison to other treatments (ALB and SIL), without affecting the crystalline content on the surface; and that UPL will improve the bond strength between Y-TZP and resin cement in comparison to traditional surface treatments (ALB and SIL) are accepted.

The results of this study could form the basis for a future projects aiming at optimizing the parameters of laser for application in different ceramic materials. In addition, testing the fatigue behavior of Y-TZP bulk material after UPL and comparison with the effects of other treatment could be valuable additions to future studies.

Acknowledgments

The Authors thank Professor Peter Herman and Dr. Jianzhao Li, Electrical and Computer Engineering, University of Toronto, for their technical help with the laser treatment, and Professor Hyeongil Kim, Biomaterials Research Laboratory at the School of Dental Medicine, University at Buffalo, for his help with samples thermocycling. This study was supported in part by a grant from Alpha Omega Foundation of Canada (Improving Bond Strength to Zirconium).

REFERENCES

[1] Bona AD, Pecho OE, Alessandretti R. Zirconia as a dental biomaterial. Materials 2015:4978–91.
[2] Guazzato M, Albakry M, Ringer SP, Swain MV. Strength, fracture toughness and microstructure of a selection of all-ceramic materials. Part II. Zirconia-based dental ceramics. Dent Mater 2004;20:449–56.
[3] Ozcan M, Bernasconi M. Adhesion to zirconia used for dental restorations: a systematic review and meta-analysis. J Adhes Dent 2015;17:7–26.
[4] Piconi C, Maccauro G. Zirconia as a ceramic biomaterial. Biomaterials 1999;20:1–25.
[5] Christel P, Meunier A, Heller M, Torre JP, Peille CN. Mechanical properties and short-term in-vivo evaluation of yttrium-oxide-partially-stabilized zirconia. J Biomed Mater Res 1989;23:45–61.
[6] Casucci A, Goracci C, Chieffi N, Monticelli F, Giovannetti A, Juloski J, et al. Microtensile bond strength evaluation of self-adhesive resin cement to zirconia ceramic after different pre-treatments. Am J Dent 2012;25:269–75.
[7] Foxton RM, Cavalcanti AN, Nakajima M, Pilecki P, Sherriff M, Melo L, et al. Durability of resin cement bond to aluminium oxide and zirconia ceramics after air abrasion and laser treatment. J Prosthodont 2011;20:84–92.
[8] Ozcan M, Cura C, Valandro LF. Early bond strength of two resin cements to Y-TZP ceramic using MPS or MPS/4-META silanes. Odontology 2011;99:62–7.
[9] Della Bona A, Donassollo TA, Demarco FF, Barrett AA, Mecholsky Jr JJ. Characterization and surface treatment effects on topography of a glass-infiltrated alumina/zirconia-reinforced ceramic. Dent Mater 2007;23:769–75.
[10] Tsuo Y, Yoshida K, Atsuta M. Effects of alumina-blasting and adhesive primers on bonding between resin luting agent and zirconia ceramics. Dent Mater J 2006;25:669–74.
[11] Blatz MB, Sadan A, Kern M. Resin-ceramic bonding: a review of the literature. J Prosthet Dent 2003;89:268–74.
[12] Spohr AM, Borges GA, Junior LH, Mota EG, Oshima HM. Surface modification of In-Ceram Zirconia ceramic by Nd:YAG laser, Rocatec system, or aluminum oxide sandblasting and its bond strength to a resin cement. Photomed Laser Surg 2008;26:203–8.
[13] Kirmali O, Kapdan A, Kustarci A, Er K. Veneer ceramic to Y-TZP bonding: comparison of different surface treatments. J Prosthodont 2016;25:324–9.
[14] Iseri U, Ozkurt Z, Yalniz A, Kazazoglu E. Comparison of different grinding procedures on the flexural strength of zirconia. J Prosthet Dent 2012;107:309–15.
[15] Ohkuma K, Kazama M, Ogura H. The grinding efficiency by diamond points developed for yttria partially stabilized zirconia. Dent Mater J 2011;30:511–6.
[16] Shahin R, Kern M. Effect of air-abrasion on the retention of zirconia ceramic crowns luted with different cements before and after artificial aging. Dent Mater 2010;26:922–8.
[17] Matinlinna JP, Choi AH, Tsoi JK. Bonding promotion of resin composite to silica-coated zirconia implant surface using a novel silane system. Clin Oral Implants Res 2013;24:290–6.
[18] Azimian F, Klosa K, Kern M. Evaluation of a new universal primer for ceramics and alloys. J Adhes Dent 2012;14:275–82.
[19] Mattiello RDL, Coelho TMK, Insaurralde E, Coelho AAK, Terra GP, Kasuya AVB, et al. A review of surface treatment methods to improve the adhesive cementation of zirconia-based ceramics. ISRN Biomater 2013;2013:10.
[20] Subasi MG, Inan O. Evaluation of the topographical surface changes and roughness of zirconia after different surface treatments. Lasers Med Sci 2012;27:735–42.
[21] Usumez A, Hamdemirci N, Koroglu BY, Simsek I, Parlar O, Sari T. Bond strength of resin cement to zirconia ceramic with different surface treatments. Lasers Med Sci 2013;28:259–66.
[22] Kasraei S, Rezaei-Soufi L, Heidari B, Vafaee F. Bond strength of resin cement to CO2 and Er:YAG laser-treated zirconia ceramic. Restor Dent Endod 2014;39:296–302.
[23] Turp V, Akgungor G, Sen D, Tuncelli B. Evaluation of surface topography of zirconia ceramic after Er:YAG laser etching. Photomed Laser Surg 2014;32:533–9.
[24] Schelle F, Polz S, Haloui H, Braun A, Dehn C, Frentzen M, et al. Ultrashort pulsed laser (USPL) application in dentistry: basic investigations of ablation rates and thresholds on oral hard tissue and restorative materials. Lasers Med Sci 2014;29:1775–83.
[25] Vicente Prieto M, Gomes ALC, Montero Martin J, Alvarado Lorenzo A, Seoane Mato V, Albaladejo Martinez A. The effect of femtosecond laser treatment on the effectiveness of resin-zirconia adhesive: an in vitro study. J Lasers Med Sci 2016;7:214–9.
[26] Fiedler S, Irsig R, Tiggesbaumker J, Schuster C, Merschjann C, Rothe N, et al. Machining of biocompatible ceramics with femtosecond laser pulses. Biomed Tech (Berl) 2013.
[27] Turp V, Sen D, Tuncelli B, Goller G, Özcan M. Evaluation of air-particle abrasion of Y-TZP with different particles using microstructural analysis. Aust Dental J 2013;58:183–91.
[28] Hallmann L, Ulmer P, Reusser E, Hämmerle CH. Effect of blasting pressure, abrasive particle size and grade on phase transformation and morphological change of dental zirconia surface. Surf Coat Technol 2012;206:4293–302.
[29] de Souza G, Hennig D, Aggarwal A, Tam LE. The use of MDP-based materials for bonding to zirconia. J Prosthet Dent 2014;112:895–902.
[30] Binnig G, Quate CF, Gerber C. Atomic force microscope. Phys Rev Lett 1986;56:930–3.
[31] Coelho A. Indexing of powder diffraction patterns by iterative use of singular value decomposition. J Appl Crystallogr 2003;36:86–95.
[32] Ko YC, Ratner BD, Hoffman AS. Characterization of hydrophilic—hydrophobic polymeric surfaces by contact angle measurements. J Colloid Interface Sci 1981;82:25–37.
[33] El-Mowafy O, El-Badrawy W, Lewis DW, Shokati B, Kermalli J, Soliman O, et al. Intensity of quartz-tungsten-halogen light-curing units used in private practice in Toronto. J Am Dent Assoc 1939;2005(136):766–73, quiz 806-7.
[34] Umino A, Nikaido T, Sultana S, Ogata M, Tagami J. Effects of smear layer and surface moisture on dentin bond strength of a waterless all-in-one adhesive. Dent Mater J 2006;25:332–8.
[35] El Zohairy AA, Saber MH, Abdalla AI, Feilzer AJ. Efficacy of microtensile versus microshear bond testing for evaluation of bond strength of dental adhesive systems to enamel. Dent Mater 2010;26:848–54.

[36] Aboushelib MN. Evaluation of zirconia/resin bond strength and interface quality using a new technique. J Adhes Dent 2011;13:255–60.
[37] Passos SP, May LG, Barca DC, Ozcan M, Bottino MA, Valandro LF. Adhesive quality of self-adhesive and conventional adhesive resin cement to Y-TZP ceramic before and after aging conditions. Oper Dent 2010;35:689–96.
[38] El-Korashy DI, El-Refai DA. Mechanical properties and bonding potential of partially stabilized zirconia treated with different chemomechanical treatments. J Adhes Dent 2014;16:365–76.
[39] Ho TK, Satterthwaite JD, Silikas N. The effect of chewing simulation on surface roughness of resin composite when opposed by zirconia ceramic and lithium disilicate ceramic. Dent Mater 2018;34:e15–24.
[40] Putra A, Chung KH, Guilherme NM, Cagna DR. Effect of bonding and Re-Bonding on the shear bond strength of two-piece implant restorations. J Prosthodont 2019;28: 305–9.
[41] Llerena-Icochea A, Costa R, Borges A, Bombonatti J, Furuse A. Bonding polycrystalline zirconia with 10-MDP–containing adhesives. Oper Dent 2017;42:335–41.
[42] Bomicke W, Schurz A, Krisam J, Rammelsberg P, Rues S. Durability of resin-zirconia bonds produced using methods available in dental practice. J Adhes Dent 2016;18:17–27.
[43] da Silva EM, Miragaya L, Sabrosa CE, Maia LC. Stability of the bond between two resin cements and an yttria-stabilized zirconia ceramic after six months of aging in water. J Prosthet Dent 2014;112:568–75.
[44] Quaas AC, Yang B, Kern M. Panavia F 2.0 bonding to contaminated zirconia ceramic after different cleaning procedures. Dent Mater 2007;23:506–12.
[45] Scherrer SS, Cattani-Lorente M, Vittecoq E, de Mestral F, Griggs JA, Wiskott HW. Fatigue behavior in water of Y-TZP zirconia ceramics after abrasion with 30 mum silica-coated alumina particles. Dent Mater 2011;27:e28–42.
[46] Cristoforides P, Amaral R, May LG, Bottino MA, Valandro LF. Composite resin to yttria stabilized tetragonal zirconia polycrystal bonding: comparison of repair methods. Oper Dent 2012;37:263–71.
[47] Miragaya L, Maia LC, Sabrosa CE, de Goes MF, da Silva EM. Evaluation of self-adhesive resin cement bond strength to yttria-stabilized zirconia ceramic (Y-TZP) using four surface treatments. J Adhes Dent 2011;13:473–80.
[48] Yang B, Barloi A, Kern M. Influence of air-abrasion on zirconia ceramic bonding using an adhesive composite resin. Dent Mater 2010;26:44–50.
[49] Thompson JY, Stoner BR, Piascik JR, Smith R. Adhesion/cementation to zirconia and other non-silicate ceramics: where are we now? Dent Mater 2011;27:71–82.
[50] Kosmac T, Oblak C, Jevnikar P, Funduk N, Marion L. Strength and reliability of surface treated Y-TZP dental ceramics. J Biomed Mater Res 2000;53:304–13.
[51] Zhang Y, Lawn BR, Malament KA, Van Thompson P, Rekow ED. Damage accumulation and fatigue life of particle-abraded ceramics. Int J Prosthodont 2006;19:442–8.
[52] Zhang Y, Lawn BR, Rekow ED, Thompson VP. Effect of sandblasting on the long-term performance of dental ceramics. J Biomed Mater Res B Appl Biomater 2004;71: 381–6.
[53] Al-Aali KA. Effect of phototherapy on shear bond strength of resin cements to zirconia ceramics: a systematic review and meta-analysis of in-vitro studies. Photodiagnosis Photodyn Ther 2018;23:58–62.
[54] Abo-Hamar SE, Hiller KA, Jung H, Federlin M, Friedl KH, Schmalz G. Bond strength of a new universal self-adhesive resin luting cement to dentin and enamel. Clin Oral Investig 2005;9:161–7.
[55] Derand T, Molin M, Kvam K. Bond strength of composite luting cement to zirconia ceramic surfaces. Dent Mater 2005;21:1158–62.
[56] Kim JH, Chae SY, Lee Y, Han GJ, Cho BH. Effects of multipurpose, universal adhesives on resin bonding to zirconia ceramic. Oper Dent 2015;40:55–62.
[57] Koizumi H, Nakayama D, Komine F, Blatz MB, Matsumura H. Bonding of resin-based luting cements to zirconia with and without the use of ceramic priming agents. J Adhes Dent 2012;14:385–92.
[58] Oyague RC, Monticelli F, Toledano M, Osorio E, Ferrari M, Osorio R. Effect of water aging on microtensile bond strength of dual-cured resin cements to pre-treated sintered zirconium-oxide ceramics. Dent Mater 2009;25:392–9.
[59] Inokoshi M, Van Meerbeek B. Adhesively luted zirconia restorations: why and how? J Adhes Dent 2014;16:294.
[60] de Oyague RC, Monticelli F, Toledano M, Osorio E, Ferrari M, Osorio R. Influence of surface treatments and resin cement selection on bonding to densely-sintered zirconium-oxide ceramic. Dent Mater 2009;25:172–9.
[61] Ohlmann B, Rammelsberg P, Schmitter M, Schwarz S, Gabbert O. All-ceramic inlay-retained fixed partial dentures: preliminary results from a clinical study. J Dent 2008;36:692–6.
[62] Rethfeld B, Sokolowski-Tinten K, von der Linde D, Anisimov SI. Timescales in the response of materials to femtosecond laser excitation. Appl Phys A 2004;79:767–9.
[63] Paranhos MP, Burnett Jr LH, Magne P. Effect of Nd:YAG laser and CO2 laser treatment on the resin bond strength to zirconia ceramic. Quintessence Int (Berl) 2011;42:79–89.
[64] Akyil MS, Uzun IH, Bayindir F. Bond strength of resin cement to yttrium-stabilized tetragonal zirconia ceramic treated with air abrasion, silica coating, and laser irradiation. Photomed Laser Surg 2010;28:801–8.
[65] Kern M. Resin bonding to oxide ceramics for dental restorations. J Adhes Sci Technol 2009;23:1097–111.
[66] Lange FF, Dunlop GL, Davis BI. Degradation during aging of transformation-toughened ZrO2-Y2O3 materials at 250°C. J Am Ceram Soc 1986;69:237–40.
[67] Hannink RH, Kelly PM, Muddle BC. Transformation toughening in zirconia-containing ceramics. J Am Ceram Soc 2000;83:461–87.
[68] Ban S, Sato H, Suehiro Y, Nakanishi H, Nawa M. Effect of sandblasting and heat treatment on biaxial flexure strength of the Zirconia/Alumina nanocomposite. Key Eng Mater 2007:330–2, 353-356.
[69] Studart AR, Filser F, Kocher P, Gauckler LJ. In vitro lifetime of dental ceramics under cyclic loading in water. Biomaterials 2007;28:2695–705.
[70] Fiedler S, Irsig R, Tiggesbaumker J, Schuster C, Merschjann C, Rothe N, et al. Machining of biocompatible ceramics with femtosecond laser pulses. Biomed Tech (Berl) 2013;58(Suppl. (1)).
[71] Gale M, Darvell B. Thermal cycling procedures for laboratory testing of dental restorations. J Dent 1999;27:89–99.
[72] Lüthy H, Loeffel O, Hammerle CH. Effect of thermocycling on bond strength of luting cements to zirconia ceramic. Dent Mater 2006;22:195–200.
[73] Gale MS, Darvell BW. Thermal cycling procedures for laboratory testing of dental restorations. J Dent 1999;27:89–99.
[74] Santerre JP, Shajii L, Leung BW. Relation of dental composite formulations to their degradation and the release of hydrolyzed polymeric-resin-derived products. Crit Rev Oral Biol Med 2001;12:136–51.
[75] Chen C, Chen Y, Lu Z, Qian M, Xie H, Tay FR. The effects of water on degradation of the zirconia-resin bond. J Dent 2017;64:23–9.

[76] Kern M, Wegner SM. Bonding to zirconia ceramic: adhesion methods and their durability. Dent Mater 1998;14:64–71.
[77] Blatz MB, Sadan A, Martin J, Lang B. In vitro evaluation of shear bond strengths of resin to densely-sintered high-purity zirconium-oxide ceramic after long-term storage and thermal cycling. J Prosthet Dent 2004;91:356–62.
[78] Phrukkanon S, Burrow MF, Tyas MJ. The influence of cross-sectional shape and surface area on the microtensile bond test. Dent Mater 1998;14:212–21.